SUPPLMENTAL FIGURES AND LEGENDS

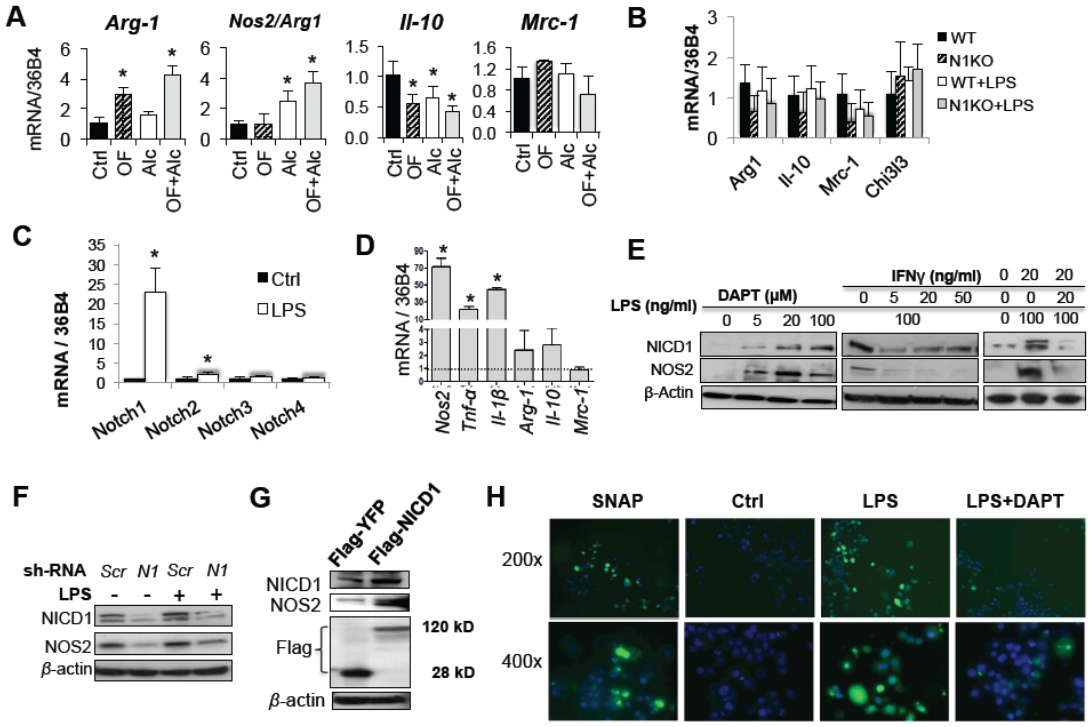

Figure S1. Notch dependent expression of M1 genes and NO production. (A) The mRNA levels of M2 (*Arg-1, Il-10, Mrc-1*) genes and the ratio of *Nos2 /Arg1* in HMac from the OF+Alc mice; n=3 to 5, * $p < 0.05$ vs. Ctrl. **(B)** Expression of M2 genes in cultured HMacs from WT and Notch1 KO mice treated with or without LPS (10 ng/ml, 4h), n=6. **(C)** The mRNA of Notch receptors 1 to 4 in Raw 264.7 cells treated with LPS for 4 h; n=3, * $p < 0.05$ vs. Ctrl. **(D)** The mRNA expression of M1 and M2 genes in Raw 264.7 cells treated with LPS for 4 h; n=3, * $p < 0.05$ compared to Ctrl (the dash line). **(E-G)** Immunoblots of NICD1 and NOS2 in Raw 264.7 cells, (**E**) treated with DAPT, followed by LPS or LPS+IFNγ for 4 h at indicated concentrations, (**F**) transduced with lentiviral *scrambled (Scr)*- or *Notch1 (N1)*- shRNA with or without LPS for 4 h, or (**G**) transiently expressed with 3x flag-YFP or 3x flag-NICD1. **(H)** Raw 264.7 cells were pretreated with or without DAPT for 16h, followed by LPS for 4 h. NO production (green) is determined with fluorescent probe DAF-FM (5μM), added 1 h after the LPS treatment. SNAP is a chemical donor of NO and serves as positive control. Statistics was done with one-way ANOVA followed by Newman-Keuls multiple comparison (A, B) and t-Test (C, D).

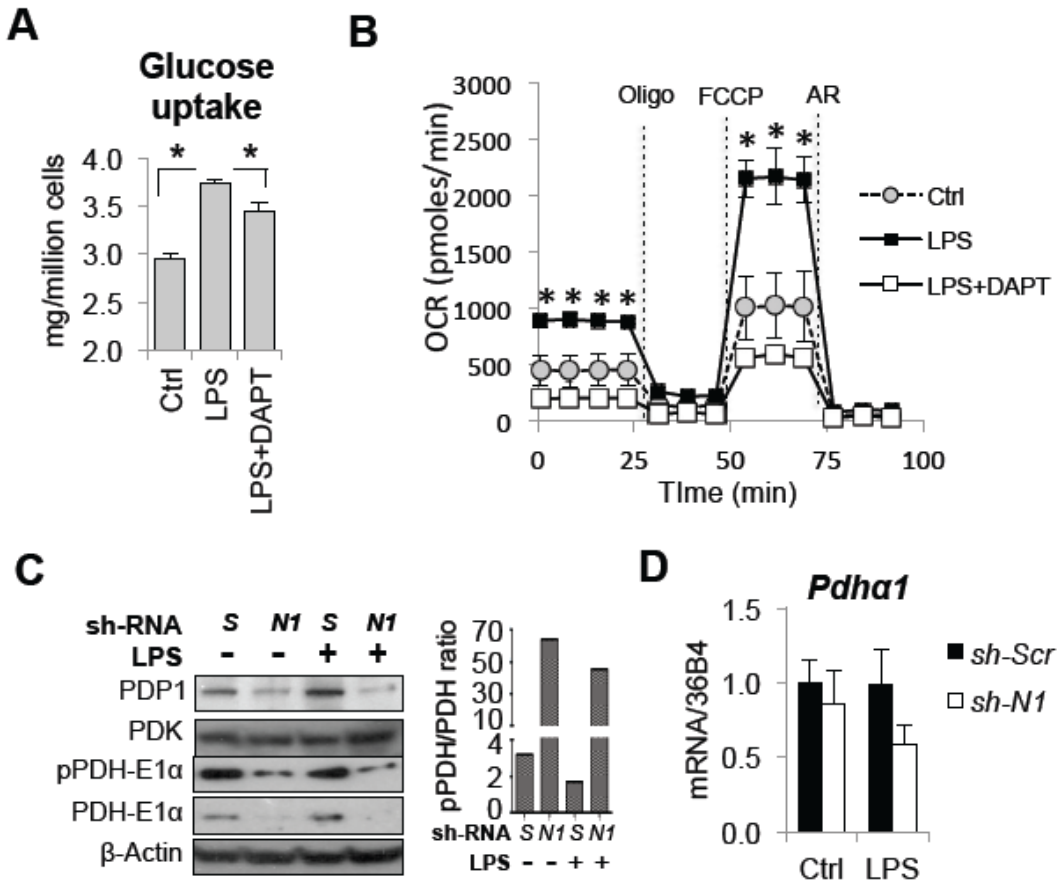

Figure S2. Notch reprograms glucose metabolism to mitochondrial oxidation in M1 Raw 264.7 cells. (A) Glucose uptake by the cells pretreated with DAPT for 4 h followed by LPS for additional 24 h; n=4, * $p<0.05$. **(B)** Cells are pretreated with or without DAPT for 16 h followed by LPS or not for 1 h, before the 3-hr Seahorse® analysis, n=4, * $p<0.05$ comparing to Ctrl or LPS+DAPT. **(C)** Immunobloting of PDP1, PDK, total- and phosphor ($pSer^{293}$)-PDH-E1α in Raw 264.7 cells infected with lentiviral *Scrambled* (*S*) *or Notch1* (*N1*) sh-RNA with or without LPS for 4h. The ratio of pPDH-E1α /PDH-E1α is shown in a bar graph. **(D)** The mRNA of pyruvate dehydrogenase E1α subunit (*Pdhα1*) in Raw 264.7 cells transduced with lentiviral *scrambled* (*Scr*) or *Notch1* (*N1*) sh-RNA, treated with or without LPS (100ng/ml) for 4 h, n=3. Statistics: one-way ANOVA (A), two-way ANOVA (D), and t-test (B).

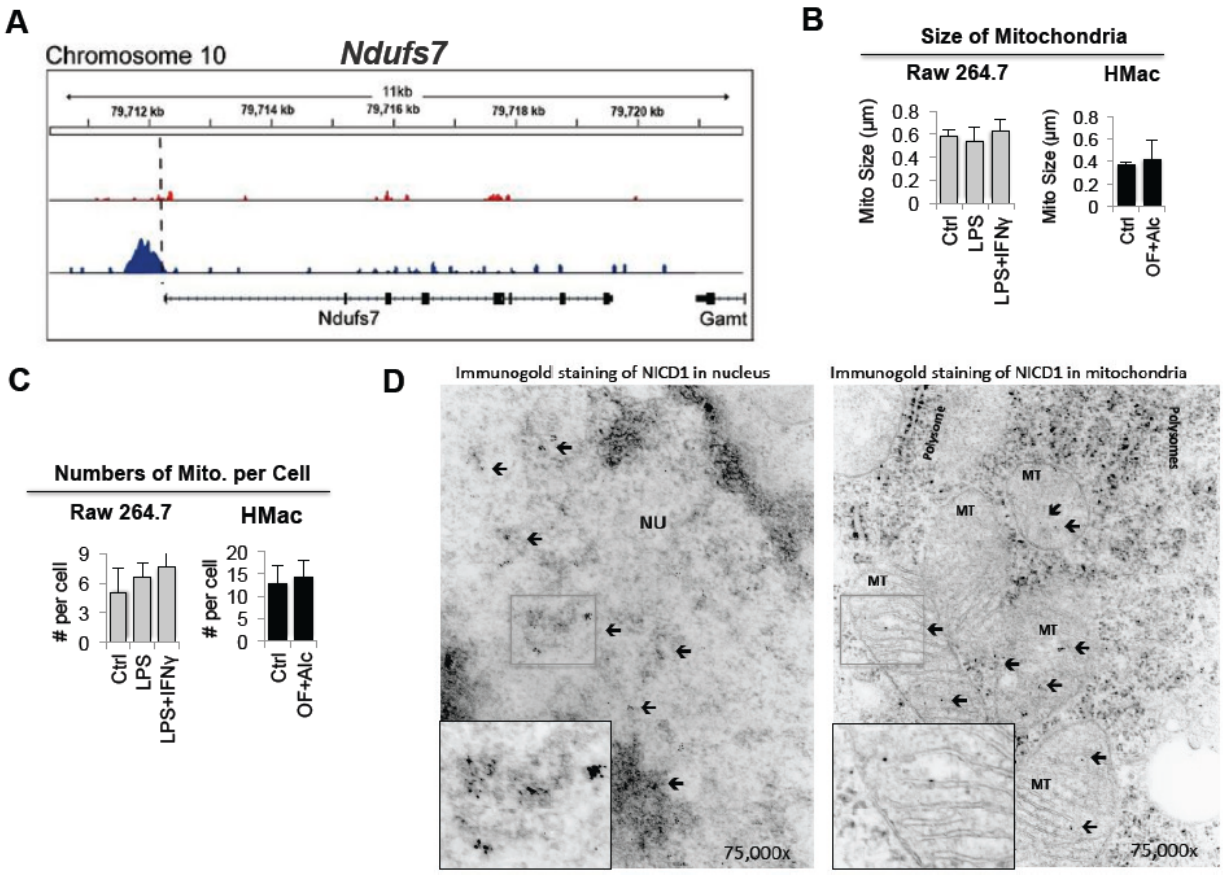

Figure S3. Notch regulates mitochondrial respiration and mtDNA transcription. (A) Integrative Genomics Viewer (IGV) genome browser tracks show a peak of Notch1 enrichment near the TSS of complex I *Ndufs7* subunit in ChIP samples (blue) over input (red). Different genomic coordinates and genome window size for *Ndufs7* (chr6:74,159,006-74,186,010; 26 kb) is shown with mm9 Reference Sequence (RefSeq) data. **(B and C)** The size (**B**) and numbers (**C**) of mitochondria in Raw 264.7 cells treated with or without LPS for 24 h, or in primary HMac from the Ctrl and OF+Alc mice, n=5-7 for both types of cells. **(D)** EM images (original 75,000x and enlarged insert 300,000x magnification) of immunogold-NICD1 localization in nucleus (NU, left panel) and in mitochondria (MT, right panel) in Raw 264.7 cells treated with or without LPS for 24 h. Statistics: one-way ANOVA for Raw 264.7 cells and t-test for HMmac in both B and C.

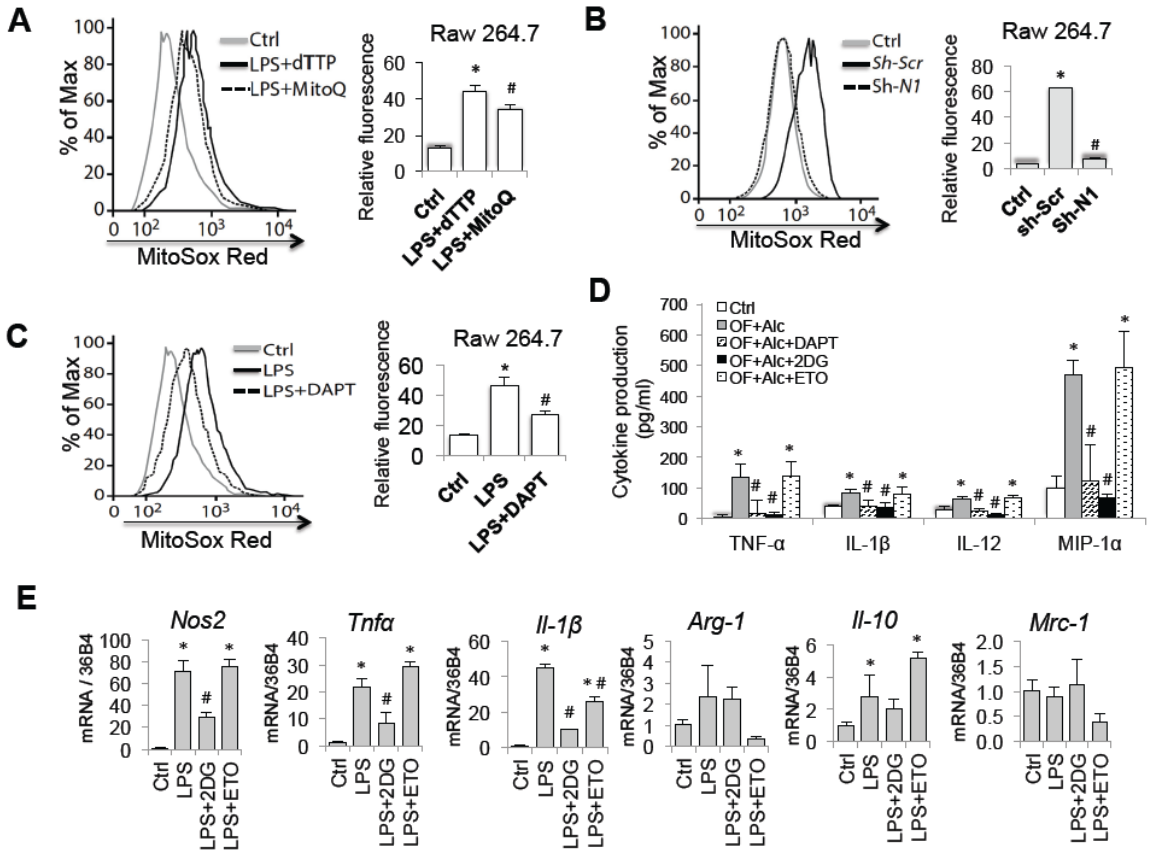

Figure S4. Notch dependent glucose oxidation and mtROS augment M1 activation. (A - C) FACS analysis of mtROS using MitoSox Red in Raw 264.7 cells, (**A**) pretreated with or without dTTP or MitoQ for 1 h followed by LPS for 24 h; dTTP served as a pharmacological control for MitoQ; (**B**) infected with *Scrambled (Scr)*- or *Notch1-shRNA* followed by LPS for 24h, or **(C)** pretreated with DAPT followed by LPS for 24h. Bar graphs depict relative fluorescence intensity; n=3-6, $p<0.01$ vs. untreated Ctrl (*) or vs. Scr-shRNA+LPS / LPS+dTTP ($^{\#}$). **(D)** 2DG and DAPT inhibit the production of proinflammatory cytokines by M1 HMac while ETO, an inhibitor of fatty acid oxidation, has no effects; n=3, $p<0.05$ vs. Ctrl (*) or OF+Alc without the inhibitors ($^{\#}$). **(E)** 2DG reduces the expression of M1 (*Nos2, Tnf-α, Il-1β)* but has minimal effects on the M2 (*Arg-1, Il-10, Mrc-1)* genes in Raw 264.7 cells treated with LPS (4 h). In contrast, ETO has minimal effects on M1 but attenuates M2 expression, n=3, $p<0.05$ vs. Ctrl (*) or LPS without the inhibitors ($^{\#}$). Statistics: one-way ANOVA for all panels.

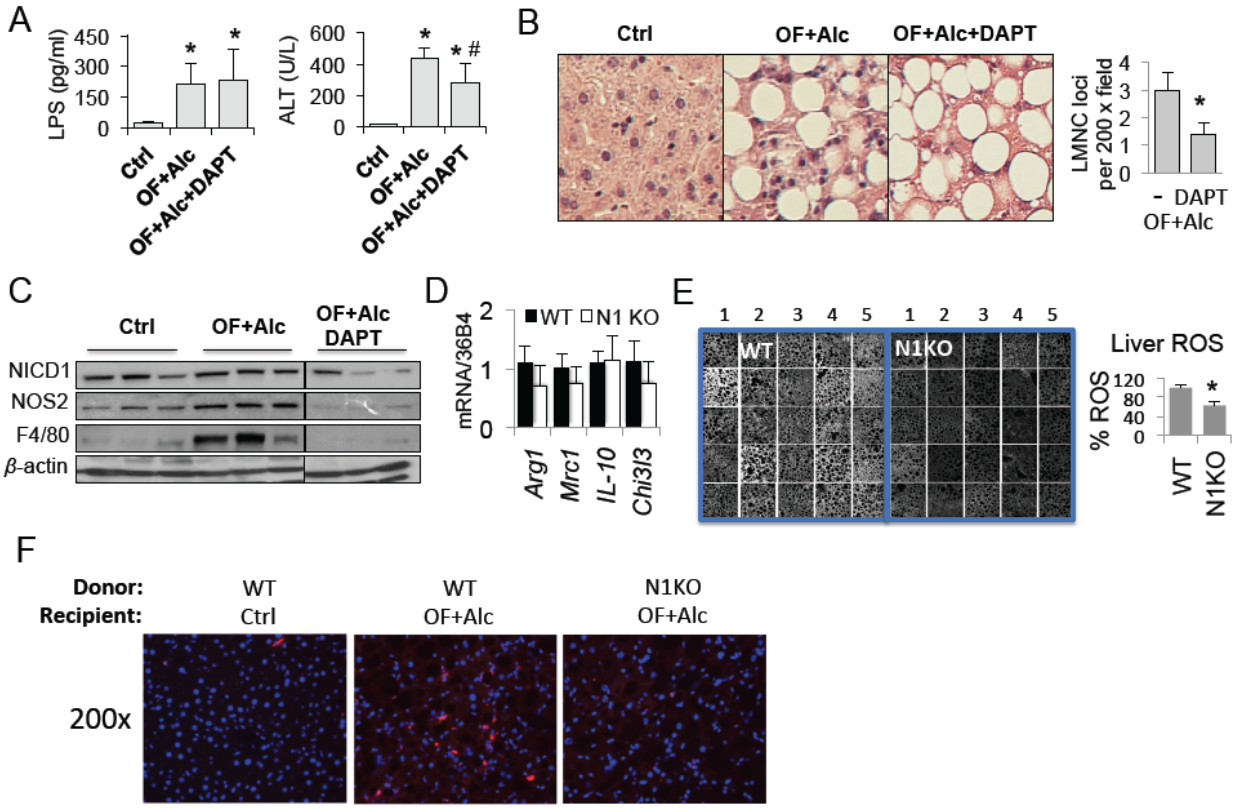

Figure S5. Inhibition of Notch pathway in vivo attenuates HMac M1 activation and liver inflammation and ROS. (A) Intraperitoneal injection of DAPT to the OF+Alc mice has no effect on portal LPS levels, but decreases plasma ALT, n = 6, $p<0.01$ vs. Ctrl (*) or OF+Alc ($^{\#}$). **(B)** Representative liver histology (H&E staining, 200x magnification) of Ctrl and OF+Alc mice with i.p. injection of DAPT or vehicle. Bar graph shows average number of loci of mononuclear cell (LMNC) per 200x optical field, n=6, * $p<0.05$. **(C)** Immunoblot of NICD1, NOS2, and F4/80 in the liver of mice with i.p. injection of DAPT or vehicle. **(D)** Expression of M2 genes in the WT and Notch1 KO HMacs subjected to OF+Alc feeding, n=3 to 5. **(E)** Liver ROS detected by DHE in the WT and Notch1 KO mice subjected to OF+Alc feeding. Total 5 random liver regions from each mouse are shown. Bar graph shows relative quantitation of fluorescent density of ROS shown in the image (200x magnification), n=5, * $p<0.05$. **(F)** Representative images of fluorescent microscopy show increased migration of PKH26 labeled (red) WT donor monocytes, but not Notch1 KO donor monocytes in the OF+Alc recipient mice compared to the control. Statistics: one-way ANOVA (A, D), t-test (B, E).

SUPPLEMENTAL TABLES

Table S1. Notch1 target nuclear genes. Genome-wide ChIP-seq was performed with chromatin fragments precipitated by anti-Notch1 antibody from the Raw 264.7 cells stimulated with LPS (100ng/ml). MACS peak calling algorithm was used to call peaks as detailed in Supplemental Methods (Bioinformatics analysis of ChIP-Seq data; $p<0.01$).

Location	Start	End	Macs Score	Dist. TSS	Type	Gene Name	Peak width
Genes with anti-microbial/pro-inflammatory function							
chr11	78734138	78734266	47.09	-158	promoter	Nos2	128
chr17	35339759	35340059	65.21	-968	promoter	Tnf	300
chr8	84927051	84927211	46.41	-687	promoter	Il15	160
chr6	113420948	113421225	56.15	-362	promoter	Il17rc	277
chr9	40812652	40812793	41.01	-53	promoter	Crtam	141
chr4	136442103	136442253	43.18	-86	promoter	C1qb	150
chr11	70958247	70958363	45.65	-99	promoter	Nlrp1a	116
chr1	74200413	74200519	47.82	-101	promoter	Cxcr2	106
chr5	65324169	65324323	42.91	-308	promoter	Tlr1	154
chr7	133560079	133560260	59.65	-1785	promoter	Cd19	181
chr2	164880768	164880879	44.58	-312	promoter	Cd40	111
chr3	96633686	96633830	50.29	-484	promoter	Cd160	144
chr8	73139794	73140007	47.4	-842	promoter	Lrrc25	213
chr4	42666458	42666560	48.75	-931	promoter	Ccl27b	102
chr6	53929783	53929900	45.44	-1185	promoter	Cpvl	117
chr1	175914107	175914219	102.44	-1188	promoter	Ifi202b	112
chr11	101900874	101901008	40.8	-1883	promoter	Cd300lg	134
chr10	90543805	90543988	42.45	-1887	promoter	Ikbip	183

Genes involved in mitochondrial function							
chr5	108863313	108863626	61.28	-72	promoter	Atp5k	313
chr10	79711698	79711847	67.96	-424	promoter	Ndufs7	149
chr19	3913870	3914100	57.84	-1268	promoter	Ndufs8	230
chr7	127778060	127778275	47.94	-535	promoter	Uqcrc2	215
chr9	21889996	21890358	44.08	-351	promoter	Ecsit	362
chr10	62407777	62407928	44.05	-1924	promoter	Dna2	151
chr9	107240703	107240866	44.58	-103	promoter	Hemk1	163
chr4	155177121	155177280	56.99	-526	promoter	Mrpl20	159
chr4	49534088	49534330	55.1	-254	promoter	Mrpl50	242
chr6	83058037	83058318	46.76	-924	promoter	Mrpl53	281
chr11	59015449	59015713	41.63	-437	promoter	Mrpl55	264
chr1	163001125	163001337	70.64	-468	promoter	Dars2	212
chr6	57486192	57486472	84.12	-912	promoter	Ppm1k	280

Table S2. TaqMan qPCR array analysis of genes of mitochondrial respiratory complexes. M1 macrophages were isolated from the liver of OF+Alc ASH mice, or obtained by the treatment of Raw 264.7 cells in vitro with LPS (100 ng/ml) + IFNγ (20 ng/ml) for 4 hours. In both cases, the cells were pretreated with the γ-secretase inhibitor DAPT or a vehicle for 16 hours. Data are presented as fold-change in expression over their respective control cells, after normalizing with the manufacturer house keeping gene 18S rRNA. **Shaded genes are transcripts of mtDNA**.

Genes	Symbol	Hepatic Macrophage		Raw 264.7	
		OF+Alc	OF+Alc +DAPT	LI	LI +DAPT
Eukaryotic 18S rRNA (Internal Control)	18S	1.00	1.00	1.00	1.00
Respiratory Complex I					
NADH dehydrogenase subunit 1	ND1	2.46	1.26	3.92	1.30
NADH dehydrogenase subunit 2	ND2	3.79	2.27	3.82	1.29
NADH dehydrogenase subunit 3	ND3	3.52	2.09	3.22	-1.08
NADH dehydrogenase subunit 4;4L	ND4;4L	1.75	-1.19	4.26	-1.23
NADH dehydrogenase subunit 5;6	ND5;ND6	4.47	1.84	4.08	1.27
NADH dehydrogenase (ubiquinone) 1 alpha subcomplex, 2	Ndufa2	2.50	1.06	1.86	-1.21
NADH dehydrogenase (ubiquinone) 1 beta subcomplex, 7	Ndufb7	2.44	-1.04	2.38	1.15
NADH dehydrogenase (ubiquinone) Fe-S protein 1	Ndufs1	2.48	-1.10	1.16	-1.16
NADH dehydrogenase (ubiquinone) flavoprotein 3	Ndufv3	2.69	-1.03	-1.23	-2.23
Respiratory Complex II					
succinate dehydrogenase complex, subunit A, flavoprotein (Fp)	Sdha	2.74	-1.03	1.47	-1.20
succinate dehydrogenase complex, subunit B, iron sulfur (Ip)	Sdhb	3.15	1.22	1.74	1.06
succinate dehydrogenase complex, subunit C, integral membrane protein	Sdhc	3.34	1.13	2.08	1.05
succinate dehydrogenase complex, subunit D, integral membrane protein	Sdhd	3.81	1.44	1.73	-1.39
Respiratory Complex III					
cytochrome b	Cytb	3.82	1.71	3.64	-1.04
cytochrome c-1	Cyc1	2.05	-1.41	1.76	1.09
ubiquinol-cytochrome c reductase core protein 1	Uqcrc1	2.60	-1.25	1.30	-1.32
Other respiratory chain components					
cytochrome c, somatic	Cycs	2.46	1.11	2.97	2.04
Respiratory Complex IV					
cytochrome c oxidase subunit I	Cox1	3.20	1.56	3.70	-1.08
cytochrome c oxidase subunit II	Cox2	3.08	1.02	3.45	-1.02
cytochrome c oxidase subunit III	Cox3	2.81	1.27	3.05	1.80
cytochrome c oxidase subunit IV isoform 1	Cox4i1	2.24	1.10	2.29	1.57
cytochrome c oxidase, subunit VIIa 2	Cox7a2	1.10	-1.47	2.47	1.21

Respiratory Complex V					
ATP synthase F0 subunit 6	ATP6	6.95	1.43	6.49	1.03
ATP synthase F0 subunit 8	ATP8	3.56	1.30	6.57	1.30
ATPase inhibitory factor 1	Atpif1	3.74	1.49	1.99	1.23
ATP synthase, H+ transporting mitochondrial F1 complex, beta subunit	Atp5b	1.95	-1.09	2.62	1.66

SUPPLEMENTAL METHODS

Materials. MitoSox Red (mitochondrial superoxide Indicator), MitoTracker Red, DAF-FM Diacetate (nitric oxide probe) were from Invitrogen; IFNγ from the R&D system; galactosamine, LPS, DAPT, and all other chemicals from Sigma-Aldrich. MitoQ10 methanesulfonate (MitoQ) and decylTPP (dTPP) were kind gifts of Professor Mike Murphy (MRC Mitochondrial Biology Unit, UK), and reviewed in reference (1).

Antibodies. Primary antibodies against following proteins are purchased commercially: NICD1 (ab8925, for western blot, confocal and electron microscopy), HIF-1α (ab2185), NF-κB p65 (ab7970), and VDAC1 (ab15895) from Abcam; Notch1 (#4380), Notch2 (#5732), Pyruvate dehydrogenase E1α (PDH, #2784), Histone H3 (#9715) and β-tubulin (#2128) from Cell Signaling; NOS2 (sc7271), PDK (sc28783), F4/80 (sc25830), CD68 (sc9139), OctA-Probe (anti-Flag, sc807), and β-actin (sc1616) from Santa Cruz Biotechnology; PDP1 (GTX109533) form GeneTex; Phospho-PDH-E1α ($pSer^{293}$, #AP1062) from Millipore, CX3CR1 (FAB5825A) from R&D systems, and CD16/32 (14016182), CD45 (12-0451), F4/80 (for FACS analysis, 17-4801) from eBiosciences. ChIP grade primary antibodies used in ChIP/ChIP-seq are from Abcam: Notch1 (ab27526), HIF-1a (ab2185), NF-kB p65 (ab7970) and RBP-Jκ (ab25949).

Primer sequences. Primer sequences used for RT-qPCR, ChIP assay.

RT-qPCR primers	Sense	Anti-sense
36B4	CACTGGTCTAGGACCCGAGAAG	GGTGCCTCTGGAGATTTTCG
Nos2	CACCAAGCTGAACTTGAGCGA	CCATAGGAAAAGACTGCACCGA
Tnf-α	ACGGCATGGATCTCAAAGAC	AGATAGCAAATCGGCTGACG
Il-1β	ACTCCTTAGTCCTCGGCCA	TGGTTTCTTGTGACCCTGAGC
Arg1	CTCCAAGCCAAAGTCCTTAGAG	AGGAGCTGTCATTAGGGACATC
Il-10	GCTCTTACTGACTGGCATGAG	CGCAGCTCTAGGAGCATGTG
Mrc-1	CTATGCAGGCCACTGCTACA	GTCTGCACCCTCCGGTACTA
Chi3l3	AGGAAGCCCTCCTAAGGACA	ACGTCAATGATTCCTGCTCC
Notch1	GTGAGGGTGATGTCAATG	TGAAGTTGAGGGAGCAGT
Notch2	ATGTGGACGAGTGTCTGTTGC	GGAAGCATAGGCACAGTCATC
Notch3	TGCCAGAGTTCAGTGGTGG	CACAGGCAAATCGGCCATC
Notch4	CTCTTGCCACTCAATTTCCCT	TTGCAGAGTTGGGTATCCCTG
Dll4	TTCCAGGCAACCTTCTCCGA	ACTGCCGCTATTCTTGTCCC
Hes1	CCGGTCTACACCAGCAACAGT	CACATGGAGTCCGAAGTGAGC
Pdp1	ATGCCAGCACCAACTCAACT	GGGTGTGTACCTCAGACGATT
Pdh1α1	GAAATGTGACCTTCATCGGCT	TGATCCGCCTTTAGCTCCATC
Pdh1α2	GTGCTGTCTCACGTATTTTCGG	GTGGCGTCGTTGGAGAACTT
ChIP primers		
Nos2 promoter CSL site	CCTCCCTCCCTAGTGAGTCC	GCAGCAGCCATCAGGTATTT
Nos2 promoter κB site	ATGGCCTTGCATGAGGATAC	CACCAAGGTGGCTGAGAAGT
Nos2 promoter HRE site	CAAGCCAGGGTATGTGGTTT	GCAGCAGCCATCAGGTATTT
Mitochondrial D-loop *	TGGGGGTAGCTAAACTGA	TGCATGACACCACAGTTA

***** These primers flank specifically the D-loop region 15752 – 15903 (151 bp) of the mtDNA (2).

Intragastric feeding mouse model. Male mice of 8-10 weeks old were given either high-fat diet (986 Cal/kg/day) or regular intake (580 Cal/kg/day) for 3 weeks. In the following 4 weeks, either Alc (for Alc and OF+Alc groups) or isocaloric dextrose (for Ctrl and OF groups) was added to the feeding regimen. At the end of the 7-week experiment, the OF and OF+Alc mice became 35-40% overweight compared to the Ctrl and Alc alone groups. Plasma ALT levels were increased in the OF (28±3 U/L) and Alc (254±46 U/L) mice, and synergistically increased to 393±29 U/L in the OF+Alc mice. The synergism in liver injury by OF+Alc was also evident by histology showing severe steatosis, mononuclear cell infiltration, and pericellular fibrosis, compared to only steatosis and moderate steatohepatitis in the OF and Alc mice, respectively. Expression of proinflammatory genes such as *Nos2* was synergistic upregulated in the liver of OF+Alc mice.

Isolation and culture of primary hepatic macrophages (HMac). HMAc were prepared by pronase/collagenase digestion and differential centrifugation as described (3), with slight modifications. Briefly, livers were sequentially perfused in situ through the portal vein at 37.5^{o}C and a flow rate of 10ml/min, with following solutions: Ca^{2+}- free MEM medium for 15 min; DMEM medium containing pronase (0.74-0.89% w/v, Roche) for 18 min; followed by DMEM medium containing type IV collagenase (0.025% w/v, Sigma) for 20 min. After perfusion, the liver was excised and dissected in DMEM containing DNase (0.8 mg/100ml, Sigma). The suspension was filtered through nylon gauze and the filtrate was centrifuged at 50 g for 2 min. The non-parenchymal cell fraction in the supernatant was collected and washed twice with DMEM, followed by centrifugation on layers of OptiPrep™ (1.085, 1.058, 1.043, and 1.034; Axis-Shield PoC As., Oslo, Norway) at 21400 rpm for 35 min at 25^{o}C. The HMac fraction was collected at the interface of 1.043/1.058 and washed with DMEM. To further purify the HMac, the cells were seeded onto Petri dishes and cultured for 1 h in DMEM medium (1000 mg/l glucose, 10% FBS). Non-adherent cells were removed by replacing media with fresh DMEM culture medium containing 3% FBS and culture overnight. The adherent HMac were collected for experiment, and the viability was determined by trypan blue exclusion and was above 90%. For pyruvate supplementation studies, HMacs were cultured first in DMEM medium containing 3% FBS for 3 hours to allow attachment to the plate. The cells were then cultured overnight in glucse/pyruvate free DMEM medium (Gibco) with or without supplementation of pyruvate (10 mM) or glucose (5.5 mM). In the next morning, the cells were treated with or without LPS (10 ng/ml) for 4 hours.

Mitochondrial ROS measurements. HMacs or Raw 264.7 cells were cultured in 12-wells plate and treated as shown in Figure Legends before incubation with MitoSOX red (to measure the mROS superoxide) at 1.0 μM for 1 hour in phonel red-free DMEM (Invitrogen) at 37 ºC. Cells

were washed with warmed PBS (37 ºC) for two times, collected with PBS containing 1mM EDTA by pipetting, and subjected to FACS analysis. The unstained cells served as negative control. The raw data were analyzed by Flowjo 6.0.

Monocyte purification, ex vivo labeling, and in vivo tracking. Mouse monocytes were from C57BL/6 WT or myeloid Notch1 KO (*LysM*-Cre:*Notch1*$^{flox/flox}$) male mice, 12 weeks of age were isolated using the EasySep Mouse Monocyte Enrichment Kit (Stemcell Tech, Canada), following the manufacturer's instructions. The isolated monocytes were labeled with PKH26 (Sigma, MO) according to the protocol by Oh *et al*. (4). The labeled monocytes were then counted and diluted in PBS. For each mouse, 0.5×10^6 cells were injected through the tail vein of the Control (n=7) or OF+Alc (n=12) mice, 5 days before the end of the 7-week feeding regimen. A piece of right-lobe liver tissue was collected for fluorescent imaging study before HMacs were isolated for FACS analysis and qRT-PCR.

To track the PKH26-labeled monocytes infiltrating to liver, the cryosection was prepared, counterstained with DAPI and visualized under the microscope and images were captured with Nikon fluorescent camera. For FACS analysis of HMacs in mice injected with PKH26 labeled monocytes, HMacs were isolated, incubated with Anti-mouse CD16/CD32 for 10 minutes on ice to block unspecific binding, and then with following antibodies: CD45-V450 (BD Biosciences), F4/80-FITC (eBio-science, San Diego, CA), and CX3CR1-APC (R&D systems) for 30 minutes, and washed 3x with cold PBS. For FACS analysis, after gating on the CD45, the PKH26+ cells were collected and PKH26- cells were further sorted into F4/80+CX3CR1^{High} - and F4/80+CX3CR1^{Low} - subsets.

Liver tissue ROS measurement. The cryosections of liver tissues collected from the control and OF+Alc mice were stained with 2μM of Dihydroethidium (Sigma, MO) for 1 hour and then washed three times with PBS. The sections were then counterstained with DAPI and visualized under the microscope and images were captured with Nikon fluorescent camera. For liver ROS quantification, immunofluorescence of Dihydroethidium staining was analyzed by Image J with five views randomly selected from each liver.

Galactosamin/LPS lethality test. Male, 3-4 months old myeloid Notch1 KO mice and their littermate controls (10 of each) were injected intraperitoneally with galactosamine (350 mg/kg) and LPS (4 μg/kg) in PBS (200 μl/mouse). The mice were monitored every two hours in the first day and every 6 hours afterwards till 48 hours. The survival curve was analyzed using GraphPad Prism software.

Immunoboloting. Cell and liver proteins were extracted in RIPA Lysis Buffer (Santa Cruz Biotechnology) containing 1mM PMSF and Halt^{TM} protease & phosphatase inhibitor cocktail

(Thermo Scientific). Nucleus proteins from cells were extracted using NE-PER™ Nuclear and Cytoplasmic Extraction Kit (Thermo Scientific). Equal amount of denatured proteins were subjected to immunobloting and visualized with chemiluminescence procedure (Roche) using the standard protocol.

qRT-PCR and TaqMan expression array. Total RNA was extracted using RNeasy Mini kit (QIAGEN) and used for synthesis of cDNA using Maxima First Strand cDNA Synthesis Kits (Thermo Scientific), which was subjected to standard SYBR green qRT-PCR analysis. The mRNA levels are relative to *36B4*. The TaqMan Expression Array was performed using 96-well customer plate with human 18s-RNA as internal standard provided by the Lifetechnologies.

Mitochondrial fractionation and purification. Cell pellets washed with PBS were re-suspended with cold MS buffer (20% sucrose, 50mM Tris-HCl, pH 7.5, 10mM EDTA) and set on ice for 10 min, followed by homogenization with a motorized pestle (3000rpm, 3x15 times) on ice. The homogenate was centrifuged at1,300g for 10 min at 4 ºC to pellet and remove nuclei. The supernatant was transferred to a fresh tube and spun at 21,000g for 15 min to pellet crude mitochondria. The pellet was re-suspended with cold MS buffer, and centrifuged through Percoll gradient layers (0%, 12%, 18%, 30%) at 37,000g for 30 min. The resulting purified mitochondria were collected from the interface of 18% and 30% Percoll layers by pipetting and transferred to a fresh tube. Mitochondria were then washed three times with 1 ml MS buffer and pelleted by centrifugation at 16,000g for 10 min. The purified mitochondria were lysed in MS buffer containing 1.0% Triton X-100, normalized by protein concentration and subjected to western blotting. Fraction purity was confirmed by blotting for the absence of Histone III (nuclei) and β-Tubulin (cytoplasm), and the presence of VDAC1 (mitochondria).

ChIP and ChIP-seq. Cells were fixed in 1% final concentration of formaldehyde. For mitochondrial ChIP, mitochondria were fractionated and purified after the formaldehyde fixation. Cells or mitochondria fractions were then sonicated to obtain 500 -1000 bp length of chromatin/mtDNA fragments, which were used for ChIP assay using the protocol provided in the ChIP Assay Kit (Millipore), or for ChIP-seq. The ChIP-seq was done by the Epigenome Center of the University of Southern California. Briefly, 200 ng of DNA were used to prepare ChIP and Input libraries, which were done similarly. To produce libraries, a protocol involving the use of the Epicentre END-IT kit, the New England Biolabs A-tailing module, and Rapid Ligase from Enyzmatics was used. Enzymatic reactions were carried out according to manufacturer's instructions. Bar-coded adapters from Bio Scientific (NEXTflex adapters) were used, and for the ChIP libraries these adapters were diluted 1:50. All cleanup steps were carried out using AMPure XP magnetic beads (Agencourt). Following adapter ligation and cleanup, one half the

amount of recovered material was subjected to 10 to 14 rounds of PCR (depending on the concentrations of the adapter-ligation material) using Kapa HiFi HotStart ReadyMix (KAPA Biosystems) and the NEXTflex amplifying primer cocktail. Following PCR, reactions were cleaned using magnetic beads and resuspended in a small volume of 10 mM Tris 8.5 (Qiagen EB). Libraries were visualized by Agilent Bioanalzyer and quantified using the Kapa Biosystems Library Quantification Kit, according to manufacturer's instructions. Enrichment for known target sequences was verified by qPCR before ChIP and input DNA were sequenced. Libraries were applied to an Illumina flow cell at a concentration of 16 pM on a version 3 flow cell and run on the HiSeq 2000 for 50 cycles. Image analysis and basecalling was carried out using RTA 1.13.48.0. Final file formatting, demultiplexing and fastq generation was carried out using CASAVA v 1.8.2.

Bioinformatics analysis of ChIP-Seq data: Approximately, 20 million reads generated were aligned with mm9 reference genome using BWA to generate around 17 million aligned reads with mapping quality ≥20 and allowing only two mismatches (5). Only one of the duplicated sequences was kept to minimize PCR artifacts. During the peak calling, a *q*-value (adjusted *P*-value calculated using Benjamini-Hochberg procedure) was set <0.05). The enriched ChIP-Seq peaks were identified using MACS (Model-based Analysis of ChIP-Seq) (6) with standard parameters $p<0.05$, mfold of 32. Peaks were annotated to promoter regions (1000 bp ± TSS) of the nearest gene using intersect function in BedTools. For processing of ChIP-seq data from mitocchoondrial fraction a different approach was used because of high background signal to noise ratio. IgG was used as negative control.

Chr M genome was divided into non-overlapping 20 bp windows and aligned reads was considered to be within a window of the midpoint of its estimated fragment. Mid-points in each window were counted, and empirical distributions of windows counts were created. Significant windows were merged if they are within 20 bp of each other. Windows with Zero counts were excluded and A zero truncated negative binomial model was used to fit the distribution and a peak with FDR adjusted $p<0.05$ were considered to be significantly enriched (7, 8). The mapping output files were also converted to browser-extensible data (BED) files. For visualization, wiggle tracks were generated and viewed in integrated genome viewer (IGV). The CHIPSeq data has been deposited in GEO as GSE, and approved by NCBI with Number GSE65151.

Immunofluorescence and confocal microscopy. Cells were grown on eight-well chamber slides, and treated with DAPT/LPS/IFNγ as described. For NO production, the cells were incubated with DAF-FM at 5.0 μM for 1 hour, fixed with 4% paraformaldehyde, and covered with

DAPI (Vector), and imaged using Nikon 5.0 immunofluoresence microscopy. For NICD1 and mitochondria co-localization, the cells were incubated with MitoTracker at 500nM for 30min, fixed with 4% paraformaldehyde, permeabilized with 0.1% Saponin in PBS for 5 min, blocked with PBS containing 5% BSA for 30 min, stained with primary antibodies (rabbit anti-NICD1 IgG from abcam, 1:100 dilution) overnight at 4 ºC, then stained with secondary antibodies (anti-rabbit IgG-FITC conjugated) for 60 min. The slides were covered with DAPI (Vector). Images were acquired with a Zeiss LSM 510 confocal microscopy at the Imaging Core of USC Liver Diseases Center. Three lasers with wavelengths of 488, 561 and 633 nm were used. The microscope was equipped with a Marzhauser motorized XY stage with joystick interface and internal 'Wide Z' motorized focus drive. The Z-stacks of images were used to confirm the intracellular location.

Immunoglod staining of NICD1 and electron microscopy. Raw 264.7 cells were stimulated with LPS (100ng/ml) for 4 hours. Cells were centrifuged and the resulting pellet was fixed in 1% Osmium Tetroxide, dehydrated with graded ethanol and propylene oxide, and embedded in epon 812. The embedded cells were sectioned for semi-thin sections (1 um) and stained with toluidine blue for observation. The ultrathin sections were then cut and mounted in 200 mesh formvar coated copper grids. Immunolabeling of the grids was accomplished by first washing the grids for 10 minutes in Wash Buffer (PBS with 1% BSA and 3% normal goat serum) and then incubated for 1 hour in primary NICD1 antibody (1:50 dilution). The grids were washed 3 times (5 minutes each) in Washing buffer, incubated for 30 minutes at room temperature with colloidal gold labeled secondary antibody (Sigma G7402, 1:40 dilution in Washing buffer). The grids were washed in PBS (5 times, 4 minutes each) and micro filtered distilled water (5 minutes). The sections were counter stained with Uranyl Acetate and Lead Citrate, and viewed using Hitachi H-600 electron microscope.

Lentiviral sh-RNA silencing. The PDP1 MISSION shRNA Lentiviral Transduction particles (#SHCLNV-XM_355470; Clone ID: TRCN000081380) was purchased from Sigma-Aldrich. The TRC mouse Notch1 shRNA (#RMM3981-201756215; Clone ID: TRCN000025908) lentiviral construct and TRC Lentiviral Non-targeting shRNA (#RHS6848, scramble) construct were purchased from Thermo Scientific Open Biosystems. All of the shRNA sequences were inserted into pLKO.1-puro vector. These lentiviral shRNA construct were used to co-transfect HEK (human embryonic kidney)-293T cells together with two packaging vectors, pCMVDR8.91 and pCMV-VSVG, using ProFection Mammalian Transfection System--Calcium Phosphate from Promega (#E1200). After 48 h, conditioned medium was collected and filtered, and the lentivirus stock was stored at −80 °C. The Raw 264.7 cells were infected with the lentivirus for 48 hours,

and then selected by puromycin (2 μg/ ml) for 7-10 days until the formation of new cell colonies. The scramble, Notch1 and PDP1 knockdown stable Raw 264.7 cell lines were maintained with puromycin (2 μg/ ml).

Morphological evaluation. Paraffin-embedded sections of liver were stained with hematoxylin and eosin using standard protocol, for the evaluation of hepatic steatosis and mononuclear cell infiltration.

Cytokine measurement. The HMac were cultured for 16 hours, and the medium was collected. The cytokines released into the medium were measured using mouse cytokine magnetic 20-Plex Panel (Life Technology) by Luminex-200 System, following the manufacturer's instruction. The levels of cytokines were normalized with the blank medium. Each assay was done in triplicates and a minimum of 3 mice were assayed in each group.

Site-directed mutagenesis and dual-luciferase reporter assay. Murine pGL2-*Nos2* promoter-Luciferase was purchased from AddGene (plasmid# 19296), which contains containing a *Nos2* promoter (-1589 to +153) between the KpnI and BglII sites. Site-directed mutagenesis on the HRE (-225 to -221), NF-κB (-86 to -76), or CSL (-72 to -67) site was performed using the QuickChange XL Site-directed Mutagenesis Kit (Agilent Technologies), with following primers,

Hre: sense: cagttttgaagtgactactttctgcctaggggccactgc

antisense: gcagtggcccctaggcagaaagtagtcacttcaaaactg

NFκB: sense: taacttgcacacccaactgtggcctcgccctttgggaacagttatg

antisense: cataactgttcccaaagggcgaggccacagttgggtgtgcaagtta

Csl sense: cccaactggggactctcccttggtgcacagttatgcaaaatagct

antisense: agctattttgcataactgtgcaccaagggagagtccccagttggg.

The mutant products are shown in the parentheses: Hre ACGTG (ACtTt), NFκB GGGGACTCTCC (GtGGcCTCgCC), and Csl TTGGGAAC (TgGtGcAC). The mutants were verified by DNA sequencing and subcloned into the pGL2 backbone vector (Promega #E1761) between HindIII and KpnI sites. For luciferase reporter assay, the wild-type or mutant *Nos2* promoter luciferase constructs and the Renilla plasmid were transfected into the wild-type or NICD1 overexpressing Raw 264.7 cells using the BioT transfection reagent (Bioland #B01-01) when the cell confluence reached 30-40%. After 32 hours, the cells were pretreated with or without DAPT (20 μM) for 16 hours, followed by LPS stimulation (100 ng/mL) for additional 4 hours. The Luciferase assay was performed using the Dual-Luciferase Assay kit (Promega #E1910). The numeric values represent the relative Firefly over the Renilla luciferase activity.

Seahorse XF-24 metabolic flux analysis. Oxygen consumption rate was measured using an XF24 extracellular analyzer (Seahorse Bioscience). The Raw 264.7 cells were pretreated with or without DAPT (20 mM) for 16 hours. HMac or Raw 264.7 cells were seeded at 100,000 cells/well density in 24-well plates for 1 hour to allow adherence to the plate. The cells were then changed to unbuffered DMEM (DMEM supplemented with 5.5 mM (for HMac) or 25 mM (for Raw 264.7 cells) glucose, 1 mM sodium pyruvate, 31 mM NaCl, 2 mM GlutaMax, pH 7.4). For Raw 264.7 cells, the medium also contained or not LPS (100 ng/ml). The HMac and the Raw 264.7 cells were incubated in a non-CO2 incubator for 1 hour. All injection reagents were adjusted to pH 7.4. Four baseline measurements were taken before sequential injection of mitochondrial inhibitors oligomycin, FCCP, and antimycin plus rotenone provided by the manufacturer (Cat# 101706-100), at final concentration of 1.5 uM each. Oxygen consumption rate was automatically calculated by the Seahorse XF-24 software. Every point represents an average of 5 different wells. The numeric values represent the oxygen consumption per 0.1 million cells.

Stable isotope based glucose flux analysis. Primary hepatic macrophages were cultured in glucose-free DMEM medium, which was reconstituted with 5.5 mM of [U-$^{13}C_6$]-glucose (99% purity, Sigma), for 24 hours. The glucose and lactate concentrations in the medium before and after the culture were determined using a glucometer and by the EnzyChrom Lactate Assay Kit (BioAssay Systems), respectively. The cells were wash 2x with ice-cold PBS, pelleted, and amino acids from the cells were extracted with glutamate further separated using ion-exchange chromatography (9). The glutamate was converted to its n-trifluoroacetyl-n-butyl ester (TAB) derivatives and subjected to mass spectrum acquisition, which was carried out using a mass selective detector (HP 5937N) connected to a gas chromatograph (HP 6890N). The inlet temperature was set at 25°C and the column (HP5) temperature was programed from 205°C to 215°C at 3°C/min. Methane was used for chemical ionization (CI) at a flow rate of 15 ml/min, and helium was used for electron impact ionization (EI) at a flow rate of 20ml/min. The glutamate-TAB derivatives were detected at m/z 356 under CI, and at m/z 198 (for C2-C5 fragment) and m/z 152 (for C2-C4 fragment) under EI. The spectrum information of these glutamate isotopomers was used to estimate the glucose flux through pyruvate dehydrogenase and pyruvate carboxylase to the TCA cycle using the method detailed previously (10).

Pyruvate dehydrogenase (PDH) activity assay. PDH enzyme activity was measured with a PDH Enzyme Activity Microplate Assay Kit (Abcam) using the protocol provided by the manufacturer. In brief, the Raw 264.7 cells stimulated with LPS (16 h) or infect with lentiviral sh-*Notch1* were harvested in cold PBS, and protein concentration was determined using the

Bradford assay. Detergent provided by the manufacture was then added to solubilize and maintain intact functional PDH. The samples were incubated on ice for 10 min, and then centrifuged at 1,000 × g for 10 min at 4°C. The supernatant was then collected and diluted to 500μg/200 μl. The diluted samples (200 μl) were added to each well of a microplate, incubated for 3 h prior to washing with a stabilizer for two times. The PDH activity was measured using the Power Wave 200 spectrophotometer (Bio-Tek Instruments) with absorbance 450 nm after 30-minute incubation with the Assay Solution.

SUPPLEMENTAL REFERENCES

1. Murphy, MP, Smith, RA. Targeting antioxidants to mitochondria by conjugation to lipophilic cations. *Annu Rev Pharmacol Toxicol*. 2007;47:629–656.
2. Johnson, RF, Witzel, II, Perkins, ND. p53-dependent regulation of mitochondrial energy production by the RelA subunit of NF-kappaB. *Cancer Res*. 2011;71(16):5588–5597.
3. Pertoft, H, Smedsrod, B. Separation and characterization of liver cells. In: Pretlow II, TG, Pretlow, TP, eds. *Cell Separation: Methods and Selected Applications*. Academic Press, London; 1987: pp. 1–24.
4. Oh, DY, Morinaga, H, Talukdar, S, Bae, EJ, Olefsky, JM. Increased macrophage migration into adipose tissue in obese mice. *Diabetes*. 2012;61(2):346–354.
5. Li, H, Durbin, R. Fast and accurate short read alignment with Burrows-Wheeler transform. *Bioinformatics*. 2009;25(14):1754–1760.
6. Zhang, Y, Liu, T, Meyer, CA, Eeckhoute, J, Johnson, DS, Bernstein, BE, Nusbaum, C, Myers, RM, Brown, M, Li, W, Liu, XS. Model-based analysis of ChIP-Seq (MACS). *Genome Biol*. 2008;9(9):R137.
7. Kharchenko, PV, Tolstorukov, MY, Park, PJ. Design and analysis of ChIP-seq experiments for DNA-binding proteins. *Nat Biotechnol*. 2008;26(12):1351–1359.
8. Rozowsky, J, Euskirchen, G, Auerbach, RK, Zhang, ZD, Gibson, T, Bjornson, R, Carriero, N, Snyder, M, Gerstein, MB. PeakSeq enables systematic scoring of ChIP-seq experiments relative to controls. *Nat Biotechnol*. 2009;27(1):66–75.
9. Katz, J, Lee, WN, Wals, PA, Bergner, EA. Studies of glycogen synthesis and the Krebs cycle by mass isotopomer analysis with [U-13C] glucose in rats. *Journal of Biological Chemistry*. 1989;264(22):12994–13004.
10. Lee, W-NP, Edmond, J, Bassilian, S, Morrow, JW. Mass isotopomer study of glutamine oxidation and synthesis in primary culture of astrocytes. *Developmental neuroscience*. 2009;18(5-6):469–477.